

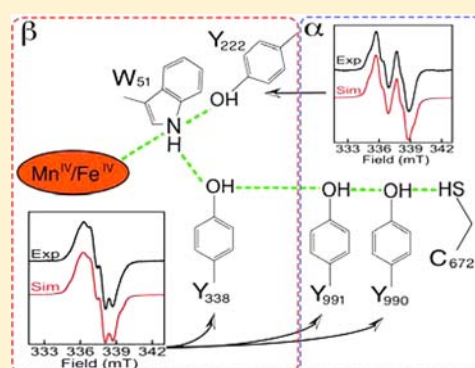
Radical-Translocation Intermediates and Hurdling of Pathway Defects in “Super-oxidized” (Mn^{IV}/Fe^{IV}) *Chlamydia trachomatis* Ribonucleotide Reductase

Laura M. K. Dassama,^{†,‡,¶} Wei Jiang,^{†,‡,¶} Paul T. Varano,[‡] Maria-Eirini Pandelia,[‡] Denise A. Conner,[‡] Jiajia Xie,[†] J. Martin Bollinger, Jr.,^{*,†,‡} and Carsten Krebs^{*,†,‡}

[†]Departments of Biochemistry and Molecular Biology and [‡]Chemistry, The Pennsylvania State University, University Park, Pennsylvania 16802, United States

S Supporting Information

ABSTRACT: A class I ribonucleotide reductase (RNR) uses either a tyrosyl radical (Y•) or a Mn^{IV}/Fe^{III} cluster in its β subunit to oxidize a cysteine residue ~35 Å away in its α subunit, generating a thiyl radical that abstracts hydrogen (H•) from the substrate. With either oxidant, the inter-subunit “hole-transfer” or “radical-translocation” (RT) process is thought to occur by a “hopping” mechanism involving multiple tyrosyl (and perhaps one tryptophanyl) radical intermediates along a specific pathway. The hopping intermediates have never been directly detected in a Mn/Fe-dependent (class Ic) RNR nor in any wild-type (wt) RNR. The Mn^{IV}/Fe^{III} cofactor of *Chlamydia trachomatis* RNR assembles via a Mn^{IV}/Fe^{IV} intermediate. Here we show that this cofactor-assembly intermediate can propagate a hole into the RT pathway when α is present, accumulating radicals with EPR spectra characteristic of Y•s. The dependence of Y• accumulation on the presence of substrate suggests that RT within this “super-oxidized” enzyme form is gated by the protein, and the failure of a β variant having the subunit-interfacial pathway Y substituted by phenylalanine to support radical accumulation implies that the Y•(s) in the wt enzyme reside(s) within the RT pathway. Remarkably, two variant β proteins having pathway substitutions rendering them inactive in their Mn^{IV}/Fe^{III} states can generate the pathway Y•s in their Mn^{IV}/Fe^{IV} states and also effect nucleotide reduction. Thus, the use of the more oxidized cofactor permits the accumulation of hopping intermediates and the “hurdling” of engineered defects in the RT pathway.



INTRODUCTION

By catalyzing conversion of ribonucleotides to 2'-deoxyribonucleotides, ribonucleotide reductases (RNRs) provide all organisms with the precursors for the *de novo* synthesis and repair of DNA.^{1,2} All known RNRs use a free-radical mechanism that is initiated by the abstraction of the hydrogen atom (H•) from the 3'-position of the nucleotide substrate by a transient cysteine thiyl radical (C•).^{3,4} The mechanism by which the C• is generated is the primary basis for the division of RNRs into classes I–III.^{1,2}

A class Ia RNR, such as the most extensively studied orthologue from aerobically growing *Escherichia coli* (*Ec*), comprises two subunits, α and β.^{1,5} Both subunits are homodimers, and they form a 1:1 complex (α₂β₂) in the active state.^{6–11} The α subunit binds substrates and effectors¹⁰ and contains the cysteine residue (C₄₃₉ in the *Ec* enzyme discussed hereafter) that forms the H•-abstracting C• during turnover.^{5,12,13} The C₄₃₉• is generated *in situ* by a stable oxidant in β. This potent oxidant, a μ-oxo-Fe₂^{III/III}/tyrosyl radical (Y•) cofactor,^{14–16} is the product of an auto-activation reaction, during which the reduced (Fe₂^{II/II}) form of the diiron cluster reacts with O₂.¹⁴ The activation reaction proceeds via a μ-

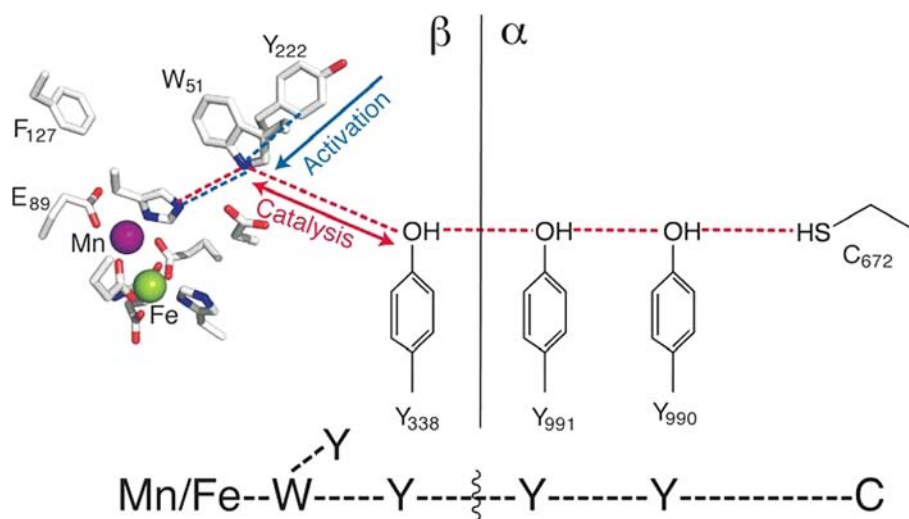
peroxo-Fe₂^{III/III} intermediate^{17,18} to a state containing both a Fe₂^{III/IV} complex, designated X, and a cation radical residing on the near-surface residue, tryptophan 48 (W₄₈).¹⁹ The W₄₈ cation radical (W₄₈⁺) can undergo rapid reduction by a number of natural compounds (e.g., ascorbate, thiols),^{19,20} leaving X to oxidize the nearby (~5 Å away) Y₁₂₂ to the Y₁₂₂• as X is reduced to the μ-oxo-Fe₂^{III/III} cluster of the active β subunit.^{21,22} The net effect of the transient oxidation of W₄₈ by the diiron–O₂ adduct and the subsequent reduction of the W₄₈⁺ from solution is the shuttling of a single electron to the buried diiron cofactor.¹⁹

The catalytic cycle of nucleotide reduction begins with the one-electron oxidation of C₄₃₉ in α by the long-lived Y₁₂₂• ~35 Å away in β upon formation of the α₂β₂ complex having the nucleoside 5'-diphosphate (NDP) substrate and (deoxy)-nucleoside triphosphate allosteric effector bound in α. The long-distance, inter-subunit radical-translocation (RT) process that generates the C₄₃₉• does not occur by a simple electron-transfer (ET) step via a tunneling mechanism. Rather, ET

Received: September 24, 2012

Published: November 16, 2012

Scheme 1. Orthogonal Activation- and Catalysis-Specific Electron-Relay Pathways in *Ct* RNR; At Bottom Is a Simple Schematic That Is Used Throughout This Work To Assist in Interpretation of the Figures



proceeds in multiple “hopping” steps involving a chain of aromatic amino acid residues (Y_{356} and perhaps W_{48} in β , and Y_{731} and Y_{730} in α), which are conserved across all class I RNRs.^{23–29} The stable Y_{122}^{\bullet} is proposed to acquire an electron from the closest pathway residue (W_{48} or Y_{356}), and the resultant “hole” is then propagated, residue-by-residue, via a series of similar hopping steps. It is thought that the individual ET steps are coupled to local proton transfers (PT), and, consequently, the term “proton-coupled electron transfer” (PCET) has been used to describe either the overall RT process or its constituent steps.^{5,11} [Note: In this article, we denote the net transfer of the hole in β to the conserved C_{439} in α as “radical translocation” (RT). “Hole hopping”, “hole translocation”, “electron relay”, and “radical transfer”, which have previously been used by us and others, have the same meaning. We disfavor “radical transfer” because the process invariably involves multiple ET events that interconvert different oxidized species (in most cases pathway radicals) rather than actual transfer of a free radical per se. We also disfavor the acronym PCET to denote the entire RT process, because the process involves multiple discrete (PC)ET events.] It is likely that, through this coupling to PT, the thermodynamics of the individual steps and the overall process are tuned for efficiency and reversibility. It is also likely that dynamic control of one or more of the required proton transfers is the mechanism by which the protein controls RT so that it occurs only in the “ready” $\beta_2\alpha_2$ -substrate-effector complex.^{28–30}

Although the mechanisms of cofactor generation and substrate reduction have been studied extensively, the crucial RT step that initiates and terminates each turnover had, until very recently, remained enigmatic, owing, in part, to the occurrence of a substrate-dependent conformational change that allows the RT process to occur along the mediating pathway.³⁰ This substrate dependence has been termed conformational “gating”, and the change that occurs in the $\alpha_2\beta_2$ complex when substrate binds as “opening of the gate”. Because the gate-opening step is slow and subsequent events are fast, the wild-type (wt) enzyme does not accumulate RT intermediates during turnover.^{5,30} In the last several years, Stubbe and co-workers have elegantly unveiled these intermediates by rational alterations to either the RT pathway

or the cofactor. They replaced key Y residues in *Ec* RNR with three different unnatural Y analogues, 3,4-dihydroxyphenylalanine (DOPA),^{8,28,31} 3-aminotyrosine (NH_2 -Y),^{8,29,32–35} and 3-nitrotyrosine (NO_2 -Y).^{36–38} The two former analogues are more easily oxidized than Y (i.e., their radicals have reduction potentials less than that of Y^{\bullet}).^{8,28,29,31–35} Effectively, their inclusion in the pathway introduces a thermodynamic depression in the hopping pathway, and the radical can then reside on this residue to a significant extent. The latter analogue was incorporated at position 122 in β , and the resultant NO_2 - Y_{122}^{\bullet} has an *elevated* reduction potential relative to the natural Y_{122}^{\bullet} .^{36,37} The presence of the more potently oxidizing initiator appeared to subvert the gating mechanism, permitting the much more rapid propagation of the radical into the pathway and the accumulation of hopping intermediates.³⁷

The class Ic RNR from *Chlamydia trachomatis* (*Ct*) differs from *Ec* RNR in that its β subunit lacks the stable, radical-initiating Y^{\bullet} .³⁹ The Y is replaced structurally by a redox-inert phenylalanine (F_{127}),^{39,40} and the function of the Y^{\bullet} is assumed by the Mn^{IV} ion of a Mn^{IV}/Fe^{III} cofactor.^{41–43} All other RT pathway residues are conserved,³⁹ suggesting that, aside from the identity of the C^{\bullet} -generating cofactor, the mechanisms of RT and nucleotide reduction might also be conserved. Analogously to cofactor assembly in *Ec* RNR, the Mn^{IV}/Fe^{III} cofactor in *Ct* RNR- β assembles in a reaction of the fully reduced cofactor form (Mn^{II}/Fe^{II}) with O_2 .⁴⁴ The reaction proceeds via a Mn^{IV}/Fe^{IV} intermediate that accumulates to near-stoichiometric yield and is sufficiently stable to permit its efficient trapping even in manual-mixing experiments.^{45,46} The intermediate is subsequently reduced by one electron at the Fe^{IV} site. The electron is shuttled through an activation-specific electron-relay pathway⁴⁷ (shown in Scheme 1) that is, to the best of our knowledge, unique to the *Ct* enzyme. This pathway comprises the surface-exposed Y_{222} (the cognate in *Ec* RNR- β is a redox-inert leucine) and W_{51} (the cognate of W_{48} in the *Ec* protein). As is the case with *Ec* RNR, no pathway RT intermediates are observed during turnover in *Ct* RNR. While efforts to incorporate unnatural amino acids into the *Ct* enzyme have thus far been unsuccessful,⁴⁸ the longevity [$t_{1/2}$ of tens of seconds at 5 °C⁴⁵] of the Mn^{IV}/Fe^{IV} cofactor assembly intermediate, itself expected to be a more potent oxidant than the native Mn^{IV}/Fe^{III} cofactor, led us to consider the

possibility that it could be used to alter the redox-potential landscape of the RT pathway to favor accumulation of radical intermediates.

Indeed, we show herein that mixing the $\text{Mn}^{\text{II}}/\text{Fe}^{\text{II}}\text{-}\beta$ complex of Ct RNR with an O_2 -containing solution of α , substrate (cytidine 5'-diphosphate, CDP), and allosteric effector (ATP) to form the $\text{Mn}^{\text{IV}}/\text{Fe}^{\text{IV}}$ activation intermediate in the presence of all other reaction components results in accumulation of EPR-active species with hyperfine couplings characteristic of Y^\bullet s. The data imply the conversion of the $\text{Mn}^{\text{IV}}/\text{Fe}^{\text{IV}}$ intermediate to a $\text{Mn}^{\text{IV}}/\text{Fe}^{\text{III}}\text{-Y}^\bullet$ species in a "super-oxidized" $\alpha_2\beta_2$ complex. Site-directed mutagenesis experiments demonstrate that the Y^\bullet resides within the RT pathway. Remarkably, two β variants with engineered RT pathway defects that render them inactive in their $\text{Mn}^{\text{IV}}/\text{Fe}^{\text{III}}$ states are, in their $\text{Mn}^{\text{IV}}/\text{Fe}^{\text{IV}}$ states, capable of both generating Y^\bullet s and promoting a single turnover of the substrate. Thus, with the more oxidized cofactor, intermediates of the RT process can be accumulated in Ct RNR, and engineered defects in the RT pathway can effectively be "hurdled" to rescue nucleotide reduction in the disabled variants.

EXPERIMENTAL PROCEDURES

Materials. Restriction enzymes and calf intestinal phosphatase were purchased from New England Biolabs (Ipswich, MA). 2-Methylbutane (*iso*-pentane), CDP, deoxycytidine 5'-diphosphate (dCDP), ATP, DTT, MgSO_4 , Dowex-1 resin, and potassium tetraborate tetrahydrate ($\text{K}_2\text{B}_4\text{O}_7\cdot 4\text{H}_2\text{O}$) were purchased from Sigma-Aldrich (St. Louis, MO). ($5\text{-}^3\text{H}$)-CDP was purchased from ViTrax (Placentia, CA). Ecoscint scintillation fluid was purchased from National Diagnostics (Atlanta, GA).

Overexpression and Purification of Ct β and Ct α . Construction of the plasmid vectors pET28a-Ct α ($\Delta 1\text{-}248$) and pET28a-Ct β expressing the wt subunits and the modified vectors expressing all the variants used in this study (except for the $\beta\text{-Y}_{222}\text{F}/\text{Y}_{338}\text{W}$ variant) has been described elsewhere.^{41,47} The vector for $\beta\text{-Y}_{222}\text{F}/\text{Y}_{338}\text{W}$ was constructed by applying a polymerase chain reaction (PCR) with the pET28a-Ct $\beta\text{-Y}_{222}\text{F}$ as the template and primers 1 (5'-TTA ACG CTT CAT ATG CAA GCA GAT ATT TTA GAT GG-3'; *NdeI* restriction site in bold) and 2 (5'-GGT GGT GCT CGA GCT ACC AAG TTA AGC TTG CTG CAT GTT GCC ATT CTA TAA CCC-3'; *XhoI* site in bold) to introduce the desired substitution (underlined). The PCR fragment was purified by agarose gel electrophoresis, restricted with *NdeI* and *XhoI*, repurified, and ligated with the larger (vector) fragment of *NdeI*- and *XhoI*-restricted pET28a-Ct β -wt. The sequence of the entire coding region of the vector was verified by ACGT, Inc. (Wheeling, IL). Purification of the N-terminally His₆-tagged proteins has also been described.^{41,47}

Synthesis of 2'-Azido-2'-deoxyuridine-5'-diphosphate Analogue ($\text{N}_3\text{-UDP}$). 2'-Azido-2'-deoxyuridine was prepared as previously described.⁴⁹ The 5'-diphosphate was appended by the method of Besada and co-workers.⁵⁰ The quantity of tributylammonium phosphate was reduced from 6 to 3 equivalents to limit formation of the *iso*-triphosphate byproducts. The identity and purity of the product were verified by comparison of its ^1H , ^{13}C , and ^{31}P NMR spectra to published data for the compound.⁴⁹⁻⁵¹

Preparation of Samples for EPR Spectroscopy. All samples (except in cases otherwise indicated) were prepared by adding 0.75 equiv of Mn^{II} and Fe^{II} to O_2 -free solutions of ~ 2 mM apo-Ct β and subsequently mixing with an air-saturated solution (hereafter referred to as " α mix") containing α , CDP (or dCDP or $\text{N}_3\text{-UDP}$), ATP, DTT, and MgSO_4 . Concentrations after mixing were 0.40 mM α , 0.20 mM β , 0.15 mM Mn, 0.15 mM Fe, 1 mM CDP (or dCDP or $\text{N}_3\text{-UDP}$), 0.5 mM ATP, 10 mM DTT, and 10 mM MgSO_4 . Samples made with CDP and dCDP were frozen in cold (~ -150 °C) 2-methylbutane 5–10 s after mixing (unless otherwise indicated), whereas samples with $\text{N}_3\text{-UDP}$ were frozen 1 min after mixing.

EPR Spectroscopy. EPR spectra were acquired on an ESP300 spectrometer equipped with a 4102ST X-band resonator and an ER 041 MR microwave bridge, all from Bruker (Billerica, MA) and described elsewhere.⁵² Cryogenic temperatures were maintained with an Oxford Instruments (Oxfordshire, UK) ESR 900 cryostat. Spectrometer conditions are provided in the figure legends. Simulation of EPR spectra of the Y^\bullet (s) was carried out with the program EasySpin.⁵³ The simulation parameters were constrained as illustrated by Svistunenko⁵⁴ and described in more detail in Supporting Information. The parameters are provided in Table S1.

"Spin" Quantification by EPR Spectroscopy. The extent of accumulation of the pathway Y^\bullet (s) was determined from analysis of the EPR spectra of duplicate samples prepared in a sequential-mix freeze-quench experiment. An O_2 -free solution of $\text{Mn}^{\text{II}}/\text{Fe}^{\text{II}}\text{-}\beta$ was first mixed with an O_2 -saturated buffer solution, and this solution was allowed to react for 2 s to form the $\text{Mn}^{\text{IV}}/\text{Fe}^{\text{IV}}$ intermediate. The pre-formed intermediate was mixed either with a solution of α , MgSO_4 , and DTT or with a solution of α , CDP, ATP, MgSO_4 , and DTT. The resultant solution was allowed to react for 1 s (ongoing studies suggest that the concentration of Y^\bullet (s) reaches its maximum value at this reaction time) before the reaction was terminated by freeze-quenching in cold (~ 120 K) 2-methylbutane. Final concentrations after mixing were 0.2 mM β , 0.15 mM Mn, 0.15 mM Fe, 0.3 mM α , 1 mM CDP (when present), 0.5 mM ATP (when present), 10 mM MgSO_4 , and 10 mM DTT. The signal intensities attributable to the $\text{Mn}^{\text{IV}}/\text{Fe}^{\text{IV}}$ intermediate and the RT pathway Y^\bullet (s) were determined from the analysis of the EPR spectra as previously described.⁵⁵ The results are summarized in Table S2.

Measurement of Product Formation with ^3H -CDP. ($5\text{-}^3\text{H}$)-CDP with specific activity >15 Ci/mmol was acquired from ViTrax (Placentia, CA). The assay procedure was adapted from that reported by Steeper and Steuart.⁵⁶ Samples were prepared so as to be identical to those used for EPR spectroscopy, with 1 mM ($5\text{-}^3\text{H}$)-CDP (~ 5000 cpm/nmol) substituted for CDP. The samples were incubated at 37 °C. Aliquots were removed at the desired reaction times, diluted 5-fold with reaction buffer (100 mM Na-HEPES, 10% v/v glycerol, pH 7.6), and quenched by incubation at 100 °C for 5 min. Quenched samples were centrifuged at 14000g for 10 min. The cleared supernatant was transferred to a clean tube, and 1 μL of 10 U/ μL calf intestinal phosphatase, 5 μL of 20 mM deoxycytidine, and 50 μL of 500 mM Tris-HCl (pH 8.5) were added. The resultant solutions were incubated for 1 h at 37 °C, and each was then loaded onto a column containing 1.5 mL of Dowex-1 resin pretreated with 0.9 M potassium tetraborate ($\text{K}_2\text{B}_4\text{O}_7\cdot 4\text{H}_2\text{O}$). The dCDP product was eluted by washing with 9 mL of distilled, deionized water. A 1 mL aliquot of the eluate was mixed with 5 mL of Ecoscint scintillation fluid; radioactivity was quantified by counting for 5 min per sample on a Beckman LS-6500 scintillation counter.

RESULTS

Initial Observation of a Possible Tyrosyl Radical (Y^\bullet) and Requirements for Its Formation. The well-characterized activation reaction of the Mn- and Fe-dependent Ct RNR β subunit begins with addition of O_2 to its $\text{Mn}^{\text{II}}/\text{Fe}^{\text{II}}$ cluster, which produces a long-lived, high-valent $\text{Mn}^{\text{IV}}/\text{Fe}^{\text{IV}}$ intermediate that decays by reduction of the Fe^{IV} ion to Fe^{III} .⁴⁵ This intermediate has unique Mössbauer- and EPR-spectroscopic features (Figure 1A, spectrum i) reflecting, first, antiferromagnetic coupling of the $S = 2$ Fe^{IV} and the $S = 3/2$ Mn^{IV} to give $S_{\text{Total}} = 1/2$ and, second, strong hyperfine coupling of the $I = 5/2$ ^{55}Mn nucleus to the electron spin.⁴⁵ The spectra of samples prepared by mixing a solution of $\text{Mn}^{\text{II}}/\text{Fe}^{\text{II}}\text{-}\beta$ with an air-saturated solution containing either α only (Figure 1A, ii) or α with the allosteric effector ATP (Figure 1A, iii) both reveal the presence of only the $\text{Mn}^{\text{IV}}/\text{Fe}^{\text{IV}}$ intermediate. By contrast, when the activation reaction is initiated by mixing the $\text{Mn}^{\text{II}}/\text{Fe}^{\text{II}}\text{-}\beta$ solution with an air-saturated solution of α and CDP

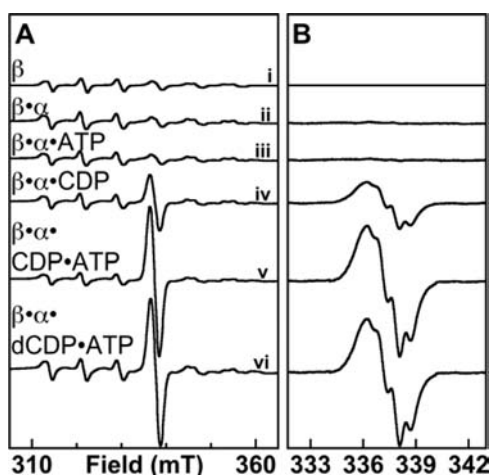


Figure 1. X-band EPR spectroscopic evidence for Y^{\bullet} accumulation in the superoxidized *Ct* RNR holoenzyme complex. At ambient temperature (22 ± 2 °C), an O_2 -free solution of β (~ 2 mM) containing 0.75 equiv each of Mn^{II} and Fe^{II} was mixed with a solution containing the other RNR reaction components to give final concentrations of 0.2 mM β ; 0 (i) or 0.4 mM α (ii–vi); 0 (i–iii) or 1 mM CDP (iv–vi); and 0 (i, ii, and iv) or 0.5 mM ATP (iii, v, and vi). Reaction solutions were transferred to an EPR tube and frozen in cold isopentane ($T \approx 125$ K) 5 s after being thoroughly mixed. (A) Delineation of the requirements for radical formation, with spectra acquired over a wide range of the magnetic field. The spectrometer conditions were $T = 14 \pm 0.2$ K, microwave frequency = 9.47 GHz, microwave power = 20 μ W, modulation frequency = 100 kHz, modulation amplitude = 10 G, time constant = 167 ms, scan time = 167 s. (B) Spectra acquired over a narrow range of the magnetic field with a smaller modulation amplitude (2 G) and 5 scans summed per spectrum to provide better resolution of the $g \approx 2$ region. In (B), the contribution of the spectrum of the Mn^{IV}/Fe^{IV} complex has been subtracted to resolve the signal of the organic radical component.

substrate, an additional signal, which overlaps with the fourth line of the spectrum of the Mn^{IV}/Fe^{IV} intermediate at $g = 2.00$, also develops (Figure 1A, iv). The signal is not observed in samples having identical composition but prepared with pre-activated β harboring the stable Mn^{IV}/Fe^{III} cofactor (Figure 3, ii). Analysis to resolve the new signal by subtraction of other spectral contributions shows that it is an organic radical that has hyperfine structure characteristic of a Y^{\bullet} (Figure 1B, iv). Although the presence of the substrate CDP is most crucial for the development of this signal, the effector ATP, while having negligible effect on its own (Figure 1, iii), appears to potentiate the effect of the substrate, resulting in greater intensity of the radical signal when both nucleotides are present (Figure 1, compare iv and v). Thus, accumulation of this radical is gated by binding of substrate and potentiated by binding of the allosteric effector in the same manner previously demonstrated for the RT step in both the *Ec* enzyme³¹ and the native form of the *Ct* enzyme.⁵⁷ Interestingly, the product, dCDP, can replace the substrate in promoting radical accumulation (Figure 1, vi).

Evidence for “Half-of-Sites Reactivity” in Radical Generation in the Super-oxidized Enzyme. The spectra of Figure 1 illustrate that accumulation of the putative $Y^{\bullet}(s)$ is in no case associated with complete decay of the Mn^{IV}/Fe^{IV} activation intermediate. This is perhaps surprising, given that the latter species is expected to generate the former species. We formulated three alternative explanations for their simultaneous presence in samples of the super-oxidized enzyme complex: (1) an equilibrium between the Mn^{IV}/Fe^{IV} -containing and $Mn^{IV}/$

$Fe^{III}-Y^{\bullet}$ -containing forms, reflecting reversibility of RT between the cluster and the Y residue(s); (2) incomplete complex formation between α and the Mn^{IV}/Fe^{IV} -containing β , which would prevent the fraction of the Mn^{IV}/Fe^{IV} cluster present in unbound β from generating a Y^{\bullet} ; and (3) half-of-sites reactivity in RT, which would prevent one of the two Mn^{IV}/Fe^{IV} clusters present in each β_2 subunit from generating a Y^{\bullet} . Explanation 1 was ruled out on the basis of the kinetics of Mn^{IV}/Fe^{IV} cluster and Y^{\bullet} decay following formation of the super-oxidized enzyme form (Figure 2A). Whereas two species in rapid equilibrium

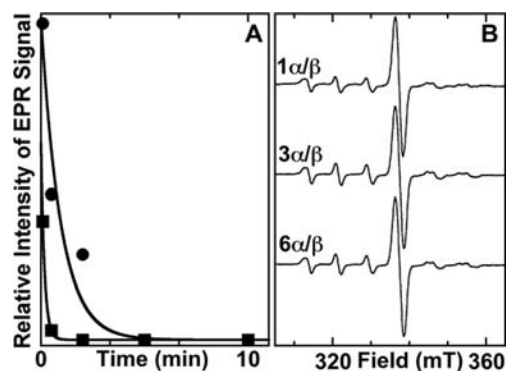


Figure 2. Tests of two possible explanations for the persistence of a fraction of the Mn^{IV}/Fe^{IV} complex even after maximal accumulation of the putative $Y^{\bullet}(s)$. (A) Kinetics of decay of the putative $Y^{\bullet}(s)$ (circles) and the Mn^{IV}/Fe^{IV} complex (squares). Traces were fit by the equation describing a single-exponential decay process, giving rate constants of 0.017 and 0.1 s^{-1} , respectively. The difference in decay rate constants rules out the possibility that the two species are in rapid equilibrium. (B) X-band EPR of samples prepared with ratios of $\alpha:\beta$ ranging from 1:1 to 6:1. Samples were prepared as described for Figure 1, except they contained 0.14 mM β and 0.14–0.84 mM α . The failures of the radical signal to increase and the Mn^{IV}/Fe^{IV} signal to be diminished rule out the possibility that weak binding between the two subunits results in a fraction of the $Mn^{IV}/Fe^{IV}-\beta$ remaining unbound and unable to generate the radical. Spectrometer conditions are the same as for Figure 1.

should develop and decay in constant proportion as a single kinetic entity, the residual Mn^{IV}/Fe^{IV} complex (squares) decays considerably (~ 6 -fold) faster than the Y^{\bullet} (circles) in these samples. As a test of explanation 2, the ratio of $\alpha:\beta$ was varied from 1:1 to 6:1, and the relative proportions of Mn^{IV}/Fe^{IV} cluster and Y^{\bullet} were assessed by EPR (Figure 2B). No significant change could be discerned with increasing $\alpha:\beta$, implying that the β subunit is almost fully saturated by α even at a 1:1 molar ratio. The results of Figure 2 thus imply that explanation 3, half-of-sites reactivity within the $\alpha_2\beta_2$ complex, is the most likely reason for the incomplete decay of the Mn^{IV}/Fe^{IV} cluster in its generation of the putative Y^{\bullet} .

To test this hypothesis further, we prepared duplicate sets of freeze-quenched EPR samples by a double-mixing protocol. A solution of $Mn^{II}/Fe^{II}-\beta$ was first mixed with O_2 -containing buffer to generate the Mn^{IV}/Fe^{IV} complex, and the intermediate was then reacted for 1 s with either α , $MgSO_4$, DTT, CDP, and ATP in the experiment or only α , $MgSO_4$, and DTT in the control. Comparison of the EPR spectra of the complete-reaction samples to those of the no-nucleotide control samples (Figure S2 and Table S2) reveals that the intensity of the EPR signature of the Mn^{IV}/Fe^{IV} intermediate decays by an average of 45%, very similar to the 50% loss expected under the assumption of half-of-sites reactivity.^{8,28,31,58,59} This lost

intensity is fully accounted for by the new $g = 2.00$ signal attributed to the $Y^{\bullet}(s)$. The spin quantification is thus completely consistent with the hypothesis that the $Y^{\bullet}(s)$ is (are) generated by the Mn^{IV}/Fe^{IV} complex on one side of each $\alpha_2\beta_2\text{ATP}\cdot\text{CDP}$ complex.

Evidence That the Radical(s) Reside(s) within the RT Pathway. Our previous work provided evidence that *Ct* RNR possesses two functionally orthogonal pathways for reduction of the Mn/Fe cluster: the activation-specific pathway, comprising Y_{222} and W_{51} of β (blue lines in Scheme 1), mediates reduction of the Fe^{IV} of the Mn^{IV}/Fe^{IV} intermediate; the catalysis-specific RT pathway, comprising Y_{338} and W_{51} of β (in addition to Y_{991} and Y_{990} of α ; red lines in Scheme 1), mediates propagation of the oxidizing equivalent from the Mn^{IV} ion of the functional Mn^{IV}/Fe^{III} cofactor to the essential C_{672} in α (the cognate of C_{439} in *Ec* α) during turnover.⁴⁷ The primary basis for identification of the latter pathway was the undetectable catalytic activities of the $W_{51}F$ and $Y_{338}F$ variants, but the importance of Y_{338} is also strongly supported by its alignment with Y_{356} of *Ec* β , which the work of Stubbe and colleagues has convincingly shown to undergo substrate-dependent, protein-gated, transient oxidation during catalysis.^{8,27,31,33,34,36–38,60} To ascertain whether the putative Y^{\bullet} detected in Figure 1 resides within the catalytic RT pathway, we substituted Y_{338} with the redox-incompetent F and tested for loss of, or changes to, the signal of the Y^{\bullet} . The EPR spectrum of a sample prepared by mixing $Mn^{II}/Fe^{II}\text{-}\beta\text{-}Y_{338}F$ with an air-saturated solution containing α , CDP, and ATP again has a radical signal at $g = 2.00$, suggestive of a Y^{\bullet} (Figure 3, iii). The signal is, however, markedly different from that observed with wt β (Figure 3, i), suggesting that the radical resides, at least in part, on a different Y residue. Previous work examining reactions of the *Ct* holoenzyme with hydroxyurea (HU) had suggested that, with Y_{338} replaced by F, substrate-dependent propagation of the oxidizing equivalent from the Mn^{IV}/Fe^{III} factor onto Y_{222} can occur, initiating HU reduction of the cofactor to the Mn^{III}/Fe^{III} state.⁵⁷ We therefore suspected that the different signal observed in the super-oxidized complex with $\beta\text{-}Y_{338}F$ might result from propagation of the oxidizing equivalent into the activation-specific pathway and onto Y_{222} . To test this possibility, we interrogated the double-variant β protein with substitutions of both Y_{338} and Y_{222} with F. The EPR spectrum of a sample prepared with this double variant lacks any signal for an organic radical (Figure 3, v). By contrast, the $Y_{222}F$ variant supports formation of a radical with an EPR spectrum very similar to that observed with wt β (Figure 3, vii). The simplest interpretation of the change in the radical EPR spectrum upon substitution of Y_{338} alone, abolition of the spectrum upon substitution of both electron-relaying Y residues in β , and absence of any effect of the $Y_{222}F$ substitution by itself is that the Y^{\bullet} observed with the wt subunit resides within the catalysis-specific RT pathway (on $\beta\text{-}Y_{338}$, $\alpha\text{-}Y_{991}$, $\alpha\text{-}Y_{990}$, or distributed among these residues) and that the $Y_{338}F$ substitution causes aberrant propagation onto Y_{222} of the activation-specific RT pathway. It is noteworthy that formation of this off-pathway (Y_{222}) radical again requires the presence of substrate. Thus, even the aberrant propagation into the activation-specific pathway still behaves (as it did in the HU study⁵⁷) as if gated by substrate binding. As previously noted, this conclusion has implications for the location and nature of the conformational gate of the RT process.

Hurdling Engineered Defects in the RT Pathway. In comparison to *Ec* Y_{356} and *Ct* Y_{338} , the roles of W_{48} of *Ec* β and

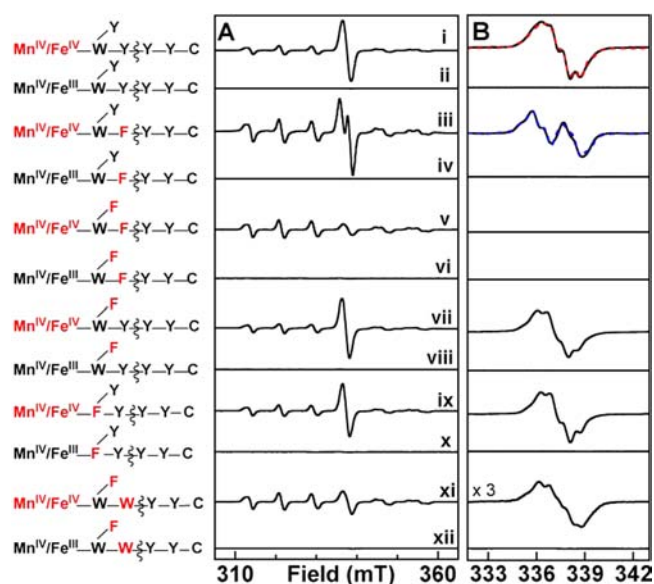


Figure 3. X-band EPR spectra illustrating the effects of substitutions of residues in the two orthogonal electron-relay pathways in *Ct* β on the nature of accumulating radical species in reactions of the $Mn^{II}/Fe^{II}\text{-}\beta$ complexes with O_2 in the presence of α , CDP, ATP, DTT, and $MgSO_4$. A schematic of the electron-relay pathways is provided at the left, with the non-native cluster redox state and substituted amino acid residues highlighted in red. Sample preparation was as described in the legend of Figure 1. For samples containing the Mn^{IV}/Fe^{III} states, each β protein was pretreated by adding air-saturated 100 mM HEPES, 10% (v/v) glycerol buffer to the $Mn^{II}/Fe^{II}\text{-}\beta$ complex and incubating for 60 min at 5 °C. This solution was then mixed with the remaining components (α , CDP, ATP, $MgSO_4$, and DTT) and frozen after ~ 5 s. (A) The “raw” experimental spectra. (B) The contribution of the Mn^{IV}/Fe^{IV} intermediate has been removed to resolve the spectra of the radical components. The red and blue dashed spectra plotted over the data in i and iii are simulations with parameters provided in Supporting Information. Spectrometer conditions are provided in the legend of Figure 1.

W_{51} of *Ct* β in catalysis are less clear. It has been established that W_{48} functions in electron relay during activation of *Ec* β : it is oxidized to a cation radical concomitantly with formation of the Y_{122}^{\bullet} -generating diiron intermediate, X.¹⁹ Moreover, the $W_{48}F$ substitution blocks ET to the cofactor in multiple contexts.^{61,62} Analogously, the $W_{51}F$ substitution in *Ct* β slows reduction of the Fe^{IV} site of the Mn^{IV}/Fe^{IV} activation intermediate.⁴⁷ Whether either W residue similarly undergoes transient oxidation during RT in *catalysis* is not yet known. To probe the role of W_{51} in the RT pathway, we tested for the ability of *Ct* $\beta\text{-}W_{51}F$ to support pathway-radical accumulation in its super-oxidized state. Remarkably, despite its incompetence for CDP reduction in the Mn^{IV}/Fe^{III} state (most likely owing to blocked RT),⁴⁷ the variant protein is fully competent for radical accumulation in its super-oxidized state (Figure 3, ix). The EPR spectrum in the $g = 2.00$ region is almost identical to that observed with wt *Ct* β . Accumulation of the radical is again dependent on the presence of the substrate CDP, suggesting proper gating of RT in the holoenzyme complex with $\beta\text{-}W_{51}F$.

The inactivity of *Ct* $\beta\text{-}W_{51}F$ in the Mn^{IV}/Fe^{III} state and competence of its Mn^{IV}/Fe^{IV} super-oxidized state to generate a pathway radical suggest that the stringency of RT-pathway structural requirements is relaxed in the super-oxidized state. As an additional test of this notion, the crucial, subunit-interfacial Y_{338} was substituted by W, a residue that might conceivably still

function in RT but with an altered redox potential. This substitution was combined with Y₂₂₂F in Ct β , so that the ability of W₃₃₈ to support pathway radical accumulation could be assessed without interference from the signal of the off-pathway Y₂₂₂[•]. Not surprisingly, the β -Y₂₂₂F/Y₃₃₈W protein lacks detectable catalytic activity in its Mn^{IV}/Fe^{III} state (the double variant is fully competent to generate this form in the reaction of its reduced enzyme form with O₂). Thus, the Y₃₃₈W substitution results in loss of proper RT with the stable Mn^{IV}/Fe^{III} cofactor. However, in the reaction of Mn^{II}/Fe^{II}- β -Y₂₂₂F/Y₃₃₈W with O₂ in the presence of α , CDP, and ATP, a radical signal does indeed develop (Figure 3, xi). The shape of the spectrum is again suggestive of a Y[•], which, if on the RT pathway, would in this case necessarily be located within α . The super-oxidized complex of this β double variant generated with the α -Y₉₉₁F variant (which readily supports radical accumulation in complex with wt β ; see Figure S1, black in the Supporting Information) lacks a significant radical signal (Figure S1, green), providing additional evidence that the radical in the β -Y₂₂₂F/Y₃₃₈W- α (wt) complex resides within α on either Y₉₉₁ or Y₉₉₀ (or perhaps distributed between them).

Functional Competence of the Y[•](s) in the Super-oxidized Ct RNR Complexes. The *raison d'être* of forward ($\beta \rightarrow \alpha$) RT within the RNR holoenzyme complex is to initiate nucleotide reduction by abstraction of H[•] from the 3' carbon of the substrate. If the Y[•] or Y[•]s observed in super-oxidized Ct RNR do, as the above evidence suggests, reside within the RT pathway, they might be expected to function in initiation of turnover. The substrate analogue, 2'-azido-2'-deoxyuridine-5'-diphosphate (N₃-UDP), can serve as a reporter of 3'-H[•] abstraction, because this step initiates a cascade of events leading to irreversible trapping of the oxidizing equivalent within α in the form of an analogue-derived radical, in which the unpaired electron spin resides primarily on a nitrogen atom derived from the azide moiety (this radical is hereafter abbreviated N[•]).^{6,63} It was previously shown that treatment of the stable, active form of β with N₃-UDP in the presence of α and ATP converts the EPR-silent Mn^{IV}/Fe^{III} cofactor to its EPR-active Mn^{III}/Fe^{III} form concomitantly with the accumulation of the N[•],⁴¹ and this observation was the key evidence establishing that the Mn^{IV}/Fe^{III} cofactor is functional in Ct RNR.⁴¹ The distinctive EPR signature of the N[•] (Figure 4, i) is partially resolved also from the spectra of the Mn^{IV}/Fe^{IV} activation intermediate and RT-pathway Y[•](s) in the super-oxidized enzyme, making the analogue potentially useful as a probe of 3'-H[•] abstraction also in this state. For the wt enzyme, interpretation would be complicated by the fact that the super-oxidized Mn^{IV}/Fe^{IV} state decays to the active Mn^{IV}/Fe^{III} form, which is itself known to support N[•] production. Thus, it would be ambiguous as to which cofactor form had been responsible for 3'-H[•] abstraction in the event that abstraction were found to occur. However, the β -W₅₁F and β -Y₂₂₂F/Y₃₃₈W variants are both inactive in their Mn^{IV}/Fe^{III} states yet capable of supporting RT-pathway Y[•] accumulation in their super-oxidized states, thereby potentially resolving this ambiguity. As expected on the basis of their incompetence for CDP reduction, neither variant supports accumulation of the N[•] when its stable Mn^{IV}/Fe^{III} state is incubated with α , ATP, and N₃-UDP (Figure 4, iii and v). Remarkably, samples prepared by mixing the Mn^{II}/Fe^{II} form of either variant with an O₂-containing solution of α , ATP, and N₃-UDP and freezing after 1 min clearly do exhibit the signature of the N[•] (Figure 4, ii and iv), thus associating the radicals observed in the super-oxidized

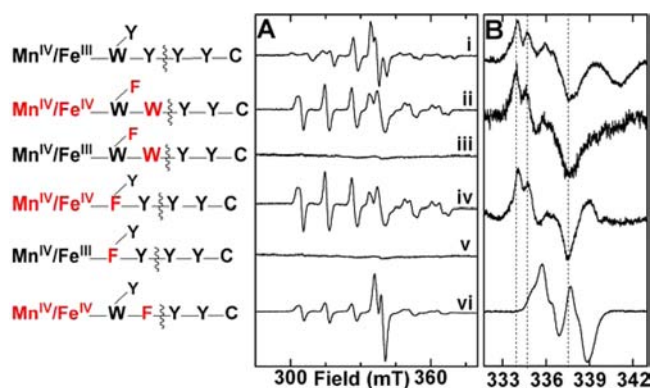


Figure 4. X-band EPR spectra of samples employing the radical-trapping substrate analogue, 2'-azido-2'-deoxyuridine-5'-diphosphate (N₃-UDP), to provide evidence for the functional competence of the RT-pathway radicals in the super-oxidized enzyme for 3'-H[•] abstraction. (A) Raw experimental spectra acquired over a wide range of the magnetic field. (B) Spectra acquired over a narrow range of the magnetic field and processed by subtraction of the contributions from either the Mn^{III}/Fe^{III} complex (i) or the Mn^{IV}/Fe^{IV} complex (ii, iv, and vi) to resolve the spectra of the organic-radical components. The method of sample preparation and the spectrometer conditions are the same as for Figures 1 and 2.

states of these RT-pathway-defective variants with successful 3'-H[•] abstraction. A control reaction employing the β -Y₃₃₈F variant, which is incompetent for accumulation of RT-pathway Y[•](s) but instead supports formation of the off-pathway Y₂₂₂[•], shows that N₃-UDP can replace CDP in the gating function, thereby supporting development of the EPR signal assigned to Y₂₂₂[•], but, as expected, does not undergo conversion to the N[•] in the holoenzyme complex with this β variant (Figure 4, vi).

The functional competence of the RT-pathway Y[•](s) was further assessed by testing directly for CDP reduction to dCDP. A published assay⁵⁶ employing tritium-labeled CDP substrate (³H-CDP, labeled at C5 of cytidine) was used to quantify the product. Background levels of radioactivity were observed in the product fractions from reactions initiated by mixing the stable Mn^{IV}/Fe^{III} forms of the β -Y₃₃₈F, β -Y₂₂₂F/Y₃₃₈W, and β -W₅₁F with α , ATP, and ³H-CDP (Figure 5, orange, black, and gray, respectively). By contrast, reactions initiated by mixing the Mn^{II}/Fe^{II} forms of the variants with O₂-containing solutions of the other reaction components (so as to generate the super-oxidized enzyme form) produced ~0.5 equiv of dCDP per β for the two variants [β -Y₂₂₂F/Y₃₃₈W (red) and β -W₅₁F (blue)] shown above to support 3'-H[•] abstraction from N₃-UDP, but gave no significant product-associated radioactivity in excess of the background for the uniformly inactive β -Y₃₃₈F variant (green). The activity profile of the variants is entirely consistent with that deduced both by EPR [accumulation of pathway Y[•](s) or absence thereof] and by use of the radical-trapping N₃-UDP analogue (production of the N[•] or failure thereto). The correlation implies that the radicals observed in the super-oxidized enzyme forms are functionally competent. The quantity of dCDP observed with the conditionally active β -Y₂₂₂F/Y₃₃₈W and β -W₅₁F variants suggests that only a single turnover can occur and that the known half-of-sites reactivity limits the super-oxidized forms to a single-turnover within just one side of the hetero-tetrameric $\alpha_2\beta_2$ complex. The conclusion of a single turnover suggests, in turn, that the bi-directionality of RT between β and α that is required for catalysis may be deranged as the enzyme operates with the

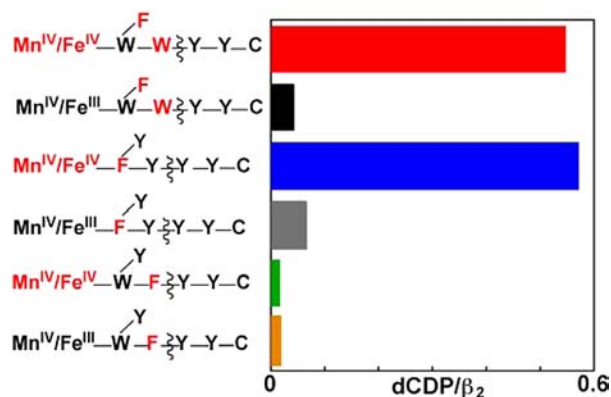


Figure 5. Product (dCDP) yields demonstrating the functional competence of RT-pathway radicals in the super-oxidized states of *Ct* β variants with pathway substitutions rendering them inactive for CDP reduction in their stable Mn^{IV}/Fe^{III} states. Reactions were initiated by mixing the indicated Mn^{II}/Fe^{II}- β complex or the pre-formed Mn^{IV}/Fe^{III}- β complex with an air-saturated solution containing the other reactions components, as in preparation of the EPR samples, but with [³H]-CDP (the site of labeling and specific activity are provided in the Experimental Procedures section) included as radioactive tracer for product quantification. After a 1-min reaction, samples were processed (as described in the procedures) based on a published method to separate substrate and product. The dCDP product was then quantified by scintillation counting.

more oxidized cofactor and RT pathway defects, thus precluding subsequent turnovers. The conclusion of a single turnover is also consistent with observations by Stubbe and co-workers on RT-pathway variants of the class Ia *Ec* RNR.^{28,37}

DISCUSSION

The characteristics of free-radical accumulation upon generation of the Mn^{IV}/Fe^{IV} activation intermediate in *Ct* RNR- β in the presence of α , a substrate (CDP), substrate analogue (N₃-UDP), or product (dCDP), and an allosteric effector (ATP) provide convincing evidence for the location of the radical(s) within the RT pathway. Radical formation requires the substrate and is potentiated by the effector, implying gating in the same manner previously demonstrated for both *Ct* and *Ec* RNR.^{28–30,57} The line shape of the $g = 2.00$ EPR signal is consistent with that of a Y[•] (with appropriate dihedral angles between the ring and C _{β} -H bonds),^{54,64} and *Ct* RNR has three Y residues (β -Y₃₃₈, α -Y₉₉₁, and α -Y₉₉₀)³⁹ that align in sequence with those shown by Stubbe and co-workers to undergo transient oxidation during catalysis by *Ec* RNR.^{27–31,37} The Y₃₃₈F substitution in β changes the EPR spectrum and thus the identity of the accumulating radical (putatively to Y₂₂₂[•]), and the combination of this substitution with the Y₂₂₂F substitution in β , which disables the activation-specific ET pathway unique to the *Ct* enzyme,⁴⁷ abolishes radical accumulation altogether. In the context of the β -Y₂₂₂F/Y₃₃₈X double variant, swapping the completely non-functional F for the potentially oxidizable W at position 338 restores radical accumulation, showing that a redox-active “stepping stone” is required at this position but need not be the native Y when the cofactor is in its super-oxidized state. By far the most compelling evidence for the location of the accumulating radicals within the RT pathway, however, is their association with 3'-H[•] abstraction: the variants that are competent for radical accumulation (β -W₅₁F and β -Y₂₂₂F/Y₃₃₈W) also support both N[•] formation from the N₃-UDP analogue and a single turnover (reduction) of CDP

substrate in their super-oxidized states, despite being essentially devoid of either activity in their stable Mn^{IV}/Fe^{III} oxidation states.

The above observations on the super-oxidized state of *Ct* RNR have some analogy to recent studies by Stubbe and co-workers examining RT and turnover in the *Ec* RNR holoenzyme complex of a β variant with the radical-harboring Y₁₂₂ replaced by 3-nitrotyrosine (NO₂-Y).³⁷ The NO₂-Y radical (NO₂-Y[•]) is a more potent oxidant (by ~200 mV) than Y[•].³⁷ As in our study, the “hot oxidant” (NO₂-Y₁₂₂[•]) was formed *in situ* in β , in this case immediately before mixing the subunits, because it is stable only for tens of seconds (half-life of ~40 s at 25 °C). Whereas turnover by the wt *Ec* enzyme initiated by Y₁₂₂[•] normally occurs at <10 s⁻¹,³⁰ owing to a rate-limiting conformational change that is probably part of the opening of the gate for Y₁₂₂[•] reduction and RT, both reduction of NO₂-Y₁₂₂[•] and dCDP production were found to be much faster in the variant [biphasic kinetics with observed first-order rate constants of ~300 and ~70 s⁻¹ for NO₂-Y₁₂₂[•] reduction and ~100 s⁻¹ for dCDP production].³⁷ The authors concluded that the more potent oxidant essentially permits hurdling of the conformational gate in a manner analogous to the hurdling of engineered pathway defects in the super-oxidized *Ct* enzyme we report in this manuscript. Their results are also consistent with the hypothesis that the gating mechanism involves dynamic control of PT to Y₁₂₂[•], because the rapid, putatively “ungated” reduction of the NO₂-Y₁₂₂[•] in the variant is *not* associated with protonation of the radical (i.e., the 3-nitrophenolate form is produced). Apparently, even without coupled PT, the initial ET from W₄₈ or Y₃₅₆ to the more potently oxidizing NO₂-Y₁₂₂[•] radical is still favorable, permitting forward RT into α . In addition, one or more new Y[•] was shown to accumulate at nearly the same rate constant as for dCDP production. More recent electron double resonance spectroscopic experiments have provided evidence that the oxidizing equivalent actually becomes distributed over Y₃₅₆ of β , Y₇₃₁ of α , and Y₇₃₀ of α ,³⁸ suggesting that the reduction potentials of the individual Y[•]s are similar. The kinetics of RT-pathway Y[•] accumulation and the location(s) of the radical(s) within the pathway in the *Ct* RNR super-oxidized state and variants thereof are actively being pursued and may shed light on the extent to which the class Ia and class Ic enzymes behave similarly in this key step.

Even without knowledge of the kinetics and precise location of the pathway radical(s), the observations on the class Ic enzyme and its super-oxidized state speak to two outstanding questions regarding the key RT step. One key question concerns the role of W₄₈/W₅₁. There is no evidence to date that either undergoes transient oxidation in RT during catalysis. The inactivity of the *Ct* β -W₅₁F variant might be taken as evidence that W₅₁ has such a role, but the absence of any evidence for a W₅₁-derived radical in the super-oxidized holoenzyme complex with the β -Y₂₂₂F/Y₃₃₈F double variant, in which radical propagation beyond W₅₁ is blocked, suggests that W₅₁ is not readily oxidized, even by the more oxidized Mn^{IV}/Fe^{IV} cofactor form. Coupled with our earlier evidence that W₅₁ is oxidized to a radical during the reaction of the Fe₂^{II/III} complex of the Y₂₂₂F variant of *Ct* β with O₂,⁴⁷ the apparent absence of any W₅₁ oxidation by the Mn^{IV}/Fe^{IV} activation intermediate can be viewed as argument against its transient oxidation during propagation of the oxidizing equivalent from the less potent Mn^{IV}/Fe^{III} cluster toward α during catalysis. A caveat to this conclusion is the possibility that oxidation of W₅₁ by the Mn/Fe cofactor (in either oxidation state) might be thermodynami-

cally disfavored, causing very little W_{51} -derived radical to accumulate, even in the super-oxidized complex of β - $Y_{222}F/Y_{338}F$. Indeed, recent work by Gray, Winkler, and co-workers has shown that electron hopping can proceed even with an element that is thermodynamically uphill by as much as 200 mV,^{65–68} which would correspond to an equilibrium between the $Mn^{IV}/Fe^{IV}-W_{51}$ and $Mn^{IV}/Fe^{III}-W_{51}^{\bullet}$ forms of the super-oxidized complex favoring the W_{51} -reduced (non-radical) form by more than 1,000-fold. Determination of the kinetics of Y^{\bullet} formation in super-oxidized *Ct* RNR and the impact of the $W_{51}F$ substitution thereupon might provide a quantitative assessment of the importance of this residue in the process.

A second outstanding question concerns the nature and location of the gate for RT. In previous work, we interpreted data on the reduction of the *Ct* RNR cofactor from the Mn^{IV}/Fe^{III} state to the Mn^{III}/Fe^{III} state by HU and the dependence thereof on the presence of the substrate and certain key electron-relaying residues as implying that the gate is adjacent to the cofactor and largely independent of the aromatic residues of the RT pathway, involving, at most, W_{51} of the pathway.⁵⁷ The observation here that the $W_{51}F$ variant supports radical accumulation, *again dependent on the presence of the substrate*, suggests that W_{51} is dispensable at least for the apparent gating being manifested by the super-oxidized enzyme. This observation would imply that the gating function is contained within the immediate vicinity of the cofactor. Intriguingly, in addition to signaling the cofactor-proximal physical gate to open, the conformational change upon substrate binding in α must have additional impact on the RT pathway in β that allows the hole to propagate outward from the cofactor into α once the gate has opened. In the absence of α , the Mn^{IV}/Fe^{IV} cluster in β must propagate a hole into the activation-specific pathway involving Y_{222} more efficiently than it does into the catalysis-specific pathway involving Y_{338} , because replacement of the former residue by F slows reduction of the Fe^{IV} site by 10–65-fold,⁴⁷ whereas substitution of the latter has *no effect* on the kinetics of Fe^{IV} -site reduction.⁵⁷ Conversely, in the holoenzyme complex, it seems that Y_{338} is oxidized to a radical in great preference to Y_{222} , and only with the former residue replaced by the redox-incompetent F does Y_{222} undergo oxidation. Thus, the conformational change in some way switches the relative reactivities of Y_{222} and Y_{338} toward one-electron oxidation.

On the basis of these observations and those by Stubbe and co-workers on their *Ec* β - $Y_{122}NO_2$ - Y variant,³⁷ our working hypothesis is that the key event in opening of the RT gate in both class Ia and class Ic RNRs is a conformational change, driven by binding of the substrate in α and propagated across the subunit interface into β , that engages the mechanism by which a proton is transferred to or within the initial oxidant (Y_{122}^{\bullet} or the $Mn^{IV}/Fe^{(III,IV)}$ cluster). This PT is coupled to ET from the cofactor proximal RT residue ($W_{48/51}$ or $Y_{356/338}$) and makes this redox step sufficiently favorable to initiate the cascade of hopping events. For the case of *Ec* RNR, our recent collaborative study with the Stubbe group has provided evidence in support of their prior suggestion that the water bound to Fe_1 of the μ -oxo- $Fe_2^{III/IV}$ cluster is the proton donor to the Y_{122}^{\bullet} oxidant.⁶⁹ Thus, it is likely that the D_{84} ligand to Fe_1 in *Ec* β , which is (i) completely conserved among class Ia orthologues but invariably replaced by E in the class Ic orthologues and (ii) in hydrogen-bonding distance from both Y_{122} and the Fe_1 water ligand in crystal structures of *Ec* β ^{15,70} mediates the crucial PT. Therefore, the gate-opening transition

could well involve re-orientation of this carboxylate ligand or enhancement of its conformational dynamics in a manner that enables its PT mediation. In consideration of this hypothesis, the behavior of the *Ec* β - $D_{84}E$ variant, which we previously showed is fully competent for cofactor assembly,⁷¹ in the holoenzyme complex becomes an intriguing issue for future examination, because it is expected that even subtle re-orientation of the carboxylate group by the presence of the additional methylene unit in the E_{84} side chain could either completely disable the crucial PT pathway or derange its conformational modulation, rendering the variant protein inactive, ungated, or both. Additionally, we⁴³ and others⁷² previously have speculated that the gate-opening step in *Ct* RNR may involve protonation of either the oxo- or hydroxobridge of the μ -oxo- μ -hydroxo-bridged Mn^{IV}/Fe^{III} cofactor.⁷³ Whether the cognate residue in *Ct* β , E_{89} , might also mediate the gatekeeping proton transfer is an open question.

■ ASSOCIATED CONTENT

📄 Supporting Information

Description of and parameters used in the simulation of the tyrosyl radicals reported in Figure 3, a schematic drawing of the phenol ring of a tyrosine residue with numerical assignments used for the simulation of the radicals, a figure demonstrating the competence of the β -wt- α - $Y_{991}F$ complex but not the β - $Y_{222}F/Y_{338}W$ - α - $Y_{991}F$ complex to form a radical, and a figure used for quantitative determination of the concentrations of the Mn^{IV}/Fe^{IV} and $Y^{\bullet}(s)$ are provided. This material is available free of charge via the Internet at <http://pubs.acs.org>.

■ AUTHOR INFORMATION

Corresponding Author

ckrebs@psu.edu; jmb21@psu.edu

Author Contributions

#L.M.K.D. and W.J. contributed equally to this work.

Notes

The authors declare no competing financial interest.

■ ACKNOWLEDGMENTS

This work was supported by the National Institutes of Health (GM-55365 to J.M.B. and C.K.) and the Alfred P. Sloan Foundation Minority Ph.D. Scholarship Program (to L.M.K.D.). The authors thank the reviewers for insightful comments.

■ REFERENCES

- (1) Nordlund, P.; Reichard, P. *Annu. Rev. Biochem.* **2006**, *75*, 681–706.
- (2) Stubbe, J. *Curr. Opin. Struct. Biol.* **2000**, *10*, 731–736.
- (3) Stubbe, J.; Ackles, D. *J. Biol. Chem.* **1980**, *255*, 8027–8030.
- (4) Mao, S. S.; Yu, G. X.; Chalfoun, D.; Stubbe, J. *Biochemistry* **1992**, *31*, 9752–9759.
- (5) Stubbe, J.; Nocera, D. G.; Yee, C. S.; Chang, M. C. Y. *Chem. Rev.* **2003**, *103*, 2167–2202.
- (6) Thelander, L.; Larsson, B.; Hobbs, J.; Eckstein, F. *J. Biol. Chem.* **1976**, *251*, 1398–405.
- (7) Brown, N. C.; Reichard, P. *J. Mol. Biol.* **1969**, *46*, 25–38.
- (8) Seyedsayamdost, M. R.; Chan, C. T. Y.; Mugnaini, V.; Stubbe, J.; Bennati, M. *J. Am. Chem. Soc.* **2007**, *129*, 15748–15749.
- (9) Thelander, L. *J. Biol. Chem.* **1973**, *248*, 4591–4601.
- (10) Uhlin, U.; Eklund, H. *Nature* **1994**, *370*, 533–539.
- (11) Reece, S. Y.; Hodgkiss, J. M.; Stubbe, J.; Nocera, D. G. *Philos. Trans. R. Soc., B* **2006**, *361*, 1351–1364.

- (12) Stubbe, J.; Riggs-Gelasco, P. *Trends Biochem. Sci.* **1998**, *23*, 438–443.
- (13) Licht, S.; Gerfen, G. J.; Stubbe, J. *Science* **1996**, *271*, 477–481.
- (14) Atkin, C. L.; Thelander, L.; Reichard, P.; Lang, G. *J. Biol. Chem.* **1973**, *248*, 7464–7472.
- (15) Nordlund, P.; Sjöberg, B.-M.; Eklund, H. *Nature* **1990**, *345*, 593–598.
- (16) Stubbe, J. *Curr. Opin. Chem. Biol.* **2003**, *7*, 183–188.
- (17) Tong, W. H.; Chen, S.; Lloyd, S. G.; Edmondson, D. E.; Huynh, B. H.; Stubbe, J. *J. Am. Chem. Soc.* **1996**, *118*, 2107–2108.
- (18) Yun, D.; García-Serres, R.; Chicaless, B. M.; An, Y. H.; Huynh, B. H.; Bollinger, J. M., Jr. *Biochemistry* **2007**, *46*, 1925–1932.
- (19) Baldwin, J.; Krebs, C.; Ley, B. A.; Edmondson, D. E.; Huynh, B. H.; Bollinger, J. M., Jr. *J. Am. Chem. Soc.* **2000**, *122*, 12195–12206.
- (20) Krebs, C.; Chen, S.; Baldwin, J.; Ley, B. A.; Patel, U.; Edmondson, D. E.; Huynh, B. H.; Bollinger, J. M., Jr. *J. Am. Chem. Soc.* **2000**, *122*, 12207–12219.
- (21) Bollinger, J. M., Jr.; Edmondson, D. E.; Huynh, B. H.; Filley, J.; Norton, J. R.; Stubbe, J. *Science* **1991**, *253*, 292–298.
- (22) Bollinger, J. M., Jr.; Stubbe, J.; Huynh, B. H.; Edmondson, D. E. *J. Am. Chem. Soc.* **1991**, *113*, 6289–91.
- (23) Ekberg, M.; Sahlin, M.; Eriksson, M.; Sjöberg, B.-M. *J. Biol. Chem.* **1996**, *271*, 20655–20659.
- (24) Ekberg, M.; Pötsch, S.; Sandin, E.; Thunnissen, M.; Nordlund, P.; Sahlin, M.; Sjöberg, B.-M. *J. Biol. Chem.* **1998**, *273*, 21003–21008.
- (25) Rova, U.; Goodtzova, K.; Ingemarson, R.; Behravan, G.; Gräslund, A.; Thelander, L. *Biochemistry* **1995**, *34*, 4267–4275.
- (26) Rova, U.; Adrait, A.; Pötsch, S.; Gräslund, A.; Thelander, L. *J. Biol. Chem.* **1999**, *274*, 23746–23751.
- (27) Seyedsayamdost, M. R.; Yee, C. S.; Reece, S. Y.; Nocera, D. G.; Stubbe, J. *J. Am. Chem. Soc.* **2006**, *128*, 1562–1568.
- (28) Seyedsayamdost, M. R.; Stubbe, J. *J. Am. Chem. Soc.* **2007**, *129*, 2226–2227.
- (29) Seyedsayamdost, M. R.; Xie, J.; Chan, C. T. Y.; Schultz, P. G.; Stubbe, J. *J. Am. Chem. Soc.* **2007**, *129*, 15060–15071.
- (30) Ge, J.; Yu, G.; Ator, M. A.; Stubbe, J. *Biochemistry* **2003**, *42*, 10017–10083.
- (31) Seyedsayamdost, M. R.; Stubbe, J. *J. Am. Chem. Soc.* **2006**, *128*, 2522–2523.
- (32) Minnihan, E. C.; Seyedsayamdost, M. R.; Stubbe, J. *Biochemistry* **2009**, *48*, 12125–12132.
- (33) Seyedsayamdost, M. R.; Argirević, T.; Minnihan, E. C.; Stubbe, J.; Bennati, M. *J. Am. Chem. Soc.* **2009**, *131*, 15729–15738.
- (34) Minnihan, E. C.; Seyedsayamdost, M. R.; Uhlin, U.; Stubbe, J. *J. Am. Chem. Soc.* **2011**, *133*, 9430–9440.
- (35) Seyedsayamdost, M. R.; Yee, C. S.; Stubbe, J. *Biochemistry* **2010**, *50*, 1403–1411.
- (36) Yokoyama, K.; Uhlin, U.; Stubbe, J. *J. Am. Chem. Soc.* **2010**, *132*, 8385–8397.
- (37) Yokoyama, K.; Uhlin, U.; Stubbe, J. *J. Am. Chem. Soc.* **2010**, *132*, 15368–15379.
- (38) Yokoyama, K.; Smith, A. A.; Corzilius, B.; Griffin, R. G.; Stubbe, J. *J. Am. Chem. Soc.* **2011**, *133*, 18420–18432.
- (39) Roshick, C.; Iliffe-Lee, E. R.; McClarty, G. *J. Biol. Chem.* **2000**, *275*, 38111–38119.
- (40) Högbom, M.; Stenmark, P.; Voevodskaya, N.; McClarty, G.; Gräslund, A.; Nordlund, P. *Science* **2004**, *305*, 245–248.
- (41) Jiang, W.; Yun, D.; Saleh, L.; Barr, E. W.; Xing, G.; Hoffart, L. M.; Maslak, M.-A.; Krebs, C.; Bollinger, J. M., Jr. *Science* **2007**, *316*, 1188–1191.
- (42) Jiang, W.; Bollinger, J. M., Jr.; Krebs, C. *J. Am. Chem. Soc.* **2007**, *129*, 7504–7505.
- (43) Bollinger, J. M., Jr.; Jiang, W.; Green, M. T.; Krebs, C. *Curr. Opin. Struct. Biol.* **2008**, *18*, 650–657.
- (44) Jiang, W.; Yun, D.; Saleh, L.; Bollinger, J. M., Jr.; Krebs, C. *Biochemistry* **2008**, *47*, 13736–13744.
- (45) Jiang, W.; Hoffart, L. M.; Krebs, C.; Bollinger, J. M., Jr. *Biochemistry* **2007**, *46*, 8709–8716.
- (46) Krebs, C.; Dassama, L. M. K.; Matthews, M. L.; Jiang, W.; Price, J. C.; Korboukh, V.; Li, N.; Bollinger, J. M., Jr. *Coord. Chem. Rev.* **2013**, *257*, 234–243.
- (47) Jiang, W.; Saleh, L.; Barr, E. W.; Xie, J.; Gardner, M. M.; Krebs, C.; Bollinger, J. M., Jr. *Biochemistry* **2008**, 8477–8484.
- (48) Stubbe, J. *Unpublished data*.
- (49) McGee, D. P. C.; Vargeese, C.; Zhai, Y.; Kirschenheuter, G. P.; Settle, A.; Siedem, C. R.; Pieken, W. A. *Nucleosides Nucleotides* **1995**, *14*, 1329–1339.
- (50) Besada, P.; Shin, D. H. *J. Med. Chem.* **2006**, *49*, 5532–5543.
- (51) Verheyden, J. P.; Wagner, D.; Moffatt, J. G. *J. Org. Chem.* **1971**, *36*, 250–254.
- (52) Price, J. C.; Barr, E. W.; Tirupati, B.; Bollinger, J. M., Jr.; Krebs, C. *Biochemistry* **2003**, *42*, 7497–7508.
- (53) Stoll, S.; Schweiger, A. *J. Magn. Reson.* **2006**, *178*, 42–55.
- (54) Svistunenko, D. A.; Cooper, C. E. *Biophys. J.* **2004**, *87*, 582–595.
- (55) Dassama, L. M. K.; Yosca, T. H.; Conner, D. A.; Lee, M. H.; Blanc, B.; Streit, B. R.; Green, M. T.; DuBois, J. L.; Krebs, C.; Bollinger, J. M., Jr. *Biochemistry* **2012**, *51*, 1607–1616.
- (56) Steeper, J. R.; Steuart, C. D. *Anal. Biochem.* **1970**, *34*, 123–130.
- (57) Jiang, W.; Xie, J.; Varano, P. T.; Krebs, C.; Bollinger, J. M., Jr. *Biochemistry* **2010**, *49*, 5340–5349.
- (58) Bennati, M.; Robblee, J. H.; Mugnaini, V.; Stubbe, J.; Freed, J. H.; Borbat, P. *J. Am. Chem. Soc.* **2005**, *127*, 15014–15015.
- (59) Uppsten, M.; Färnegårdh, M.; Domkin, V.; Uhlin, U. *J. Mol. Biol.* **2006**, *359*, 365–377.
- (60) Yee, C. S.; Seyedsayamdost, M. R.; Chang, M. C. Y.; Nocera, D. G.; Stubbe, J. *Biochemistry* **2003**, *42*, 14541–14552.
- (61) Parkin, S. E.; Chen, S.; Ley, B. A.; Mangravite, L.; Edmondson, D. E.; Huynh, B. H.; Bollinger, J. M., Jr. *Biochemistry* **1998**, *37*, 1124–1130.
- (62) Baldwin, J.; Voegtli, W. C.; Khidekel, N.; Moënné-Loccoz, P.; Krebs, C.; Pereira, A. S.; Ley, B. A.; Huynh, B. H.; Loehr, T. M.; Riggs-Gelasco, P. J.; Rosenzweig, A. C.; Bollinger, J. M., Jr. *J. Am. Chem. Soc.* **2001**, *123*, 7017–7030.
- (63) Fritscher, J.; Artin, E.; Wnuk, S.; Bar, G.; Robblee, J. H.; Kacprzak, S.; Kaupp, M.; Griffin, R. G.; Bennati, M.; Stubbe, J. *J. Am. Chem. Soc.* **2005**, *127*, 7729–7738.
- (64) Bender, C. J.; Sahlin, M.; Babcock, G. T.; Barry, B. A.; Chandrashekar, T. K.; Salowe, S. P.; Stubbe, J.; Lindström, B.; Petersson, L.; Ehrenberg, A.; Sjöberg, B.-M. *J. Am. Chem. Soc.* **1989**, *111*, 8076–8083.
- (65) Gray, H. B.; Winkler, J. R. *Q. Rev. Biophys.* **2003**, *36*, 341–376.
- (66) Gray, H. B.; Winkler, J. R. *Biochim. Biophys. Acta* **2010**, *1797*, 1563–1572.
- (67) Shih, C.; Museth, A. K.; Abrahamsson, M.; Blanco-Rodriguez, A. M.; Di Bilio, A. J.; Sudhamsu, J.; Crane, B. R.; Ronayne, K. L.; Towrie, M.; Vlček, A., Jr.; Richards, J. H.; Winkler, J. R.; Gray, H. B. *Science* **2008**, *320*, 1760–1762.
- (68) Warren, J. J.; Ener, M. E.; Vlček, A., Jr.; Winkler, J. R.; Gray, H. B. *Coord. Chem. Rev.* **2012**, *256*, 2478–2487.
- (69) Wörsdörfer, B.; Conner, D. A.; Yokoyama, K.; Seyedsayamdost, M. R.; Jiang, W.; Stubbe, J.; Bollinger, J. M., Jr.; Krebs, C. Submitted, 2012.
- (70) Högbom, M.; Galander, M.; Andersson, M.; Kolberg, M.; Hofbauer, W.; Lassmann, G.; Nordlund, P.; Lendzian, F. *Proc. Natl. Acad. Sci. U.S.A.* **2003**, *100*, 3209–3214.
- (71) Bollinger, J. M., Jr.; Krebs, C.; Vicol, A.; Chen, S.; Ley, B. A.; Edmondson, D. E.; Huynh, B. H. *J. Am. Chem. Soc.* **1998**, *120*, 1094–1095.
- (72) Roos, K.; Siegbahn, P. E. M. *Biochemistry* **2009**, *48*, 1878–1887.
- (73) Younker, J. M.; Krest, C. M.; Jiang, W.; Krebs, C.; Bollinger, J. M., Jr.; Green, M. T. *J. Am. Chem. Soc.* **2008**, *130*, 15022–15027.